Model for particle production in nuclear reactions at intermediate energies: Application to C-C collisions at 95 MeV/nucleon

J. Dudouet and D. Durand
LPC Caen, ENSICAEN, Université de Caen, CNRS/IN2P3, Caen, France
(Received 4 February 2016; revised manuscript received 8 June 2016; published 27 July 2016)

A model describing nuclear collisions at intermediate energies is presented and the results are compared with recently measured double differential cross sections in C-C reactions at 95 MeV/nucleon. Results show the key role played by geometrical effects and the memory of the entrance channel, in particular the momentum distributions of the two incoming nuclei. Special attention is paid to the description of processes occurring at midrapidity. To this end, a random particle production mechanism by means of a coalescence process in velocity space is considered in the overlap region of the two interacting nuclei.

DOI: 10.1103/PhysRevC.94.014616

I. INTRODUCTION

In a previous paper [1], the available nuclear collision models implemented in the GEANT4 toolkit [2] were "benchmarked" with the help of a comparison with experimental data obtained in C-C reactions at 95 MeV/nucleon [3,4]. Results of that work showed discrepancies between the models and the data. In particular, it revealed some difficulties in reproducing correctly the so-called midrapidity region, i.e., the kinematical region in between the projectile and the target velocities. The models implemented in GEANT4 are all dynamical models often coupled to an evaporation model that treats secondary decays. The discrepancies at midrapidity are linked to the difficulty of reproducing the production and the kinematics of light clusters produced by the mixing of nucleons originated from both projectile and target. In the present work, we present a model called SLIIPIE (simulations of light ions induced processes at intermediate energies) with some hypotheses that could help improve this point. In particular, we consider a scenario in which clusters are produced very rapidly well before the system reaches equilibrium. This is achieved by considering an almost "instantaneous" aggregation based on the initial conditions of the reaction as first proposed in [5].

II. MODEL ASSUMPTIONS

A main feature of the model is based on a strict geometrical assumption similar to the so-called participant-spectator model which is widely used at higher energies. This means that for a given impact parameter, the nucleons are shared among three different species, the quasiprojectile (quasitarget) made of nucleons belonging to the projectile (target) and not belonging to the overlap geometrical region between the two partners and the participant zone made of nucleons belonging to the overlap region.

We also consider a two-step semimicroscopic model related to two different time scales of the reaction. In a first short step, the so-called entrance channel, particle and excited fragment production occur. In a second step, the exit channel, on a larger time scale (typically of several tens of fm/c and at times much larger than the reaction time), excited species decay by particle emission and this is considered using the usual statistical decay theory. By semimicroscopic, we mean that the degrees of freedom of the model are considered at both microscopic and macroscopic levels. At the microscopic level, the internal momentum and spatial distributions of the nucleons of the two incoming nuclei are considered. At the macroscopic level, the collision is simulated by means of geometrical assumptions and macroscopic quantities such as excitation energies are estimated using "by hand" prescriptions. At variance with fully dynamical models such as the intranuclear cascade, quantum molecular dynamics approaches [6], semiclassical transport models [7] that consider the time evolution of the ensemble of nucleons, a major aspect of the present model is based on what we could call a sudden and frozen approximation. It is indeed assumed that particle and fragment production occurs on such a very short time scale that the momentum distributions of the incoming nuclei have no time to fully relax and are only affected initially by a given amount of hard in-medium nucleon-nucleon collisions. As such, the kinematical characteristics of the particle and the fragments at their time of production are entirely determined by the almost unperturbed and frozen initial nucleon distribution and thus keep a strong memory of the entrance channel of the reaction.

A. Entrance channel modeling

1. Initial conditions

The initialization procedure consists of preparing the two incoming nuclei before treating the collision itself. In particular, the internal momentum distribution is built based on well-known shell-model distributions:

$$\frac{dN}{d\mathrm{p}} = \left[1 + \frac{(A-4)\, b_0\, \mathrm{p}^2}{6}\right] \mathrm{p}^2 e^{-b_0 \mathrm{p}^2}, \tag{1}$$

where A is the mass and $b_0 = 68.5 \times 10^{-6}$ $(\mathrm{MeV}/c)^{-2}$ [8,9]. Similar distributions are used for both protons and neutrons. A center-of-mass correction is applied to ensure that the initial nuclei are at rest. Then, the projectile distribution is boosted in the laboratory frame.

Each impact parameter b is sampled between $b = 0$ and $b_{\max}$, $b_{\max}$ being the sum of the radius R of two partners of the

reaction [10]

$$R = 1.28A^{1/3} - 0.76 + 0.8A^{-1.3}\ (\text{fm}), \tag{2}$$

where A is the mass number of the nucleus. The overlap function of the projectile and the target is calculated by Monte Carlo based on well-known density distributions. From the overlap function, it is thus possible to determine the size of the quasiprojectile A_{QP} and of the quasitarget A_{QT}. The remaining nucleons constitute the participant zone (PZ). Let us call $A^{\text{PZ}}_{\text{proj}}$ and $A^{\text{PZ}}_{\text{targ}}$ the number of nucleons in PZ, respectively, from the projectile and target. We have $A^{\text{PZ}} = A^{\text{PZ}}_{\text{proj}} + A^{\text{PZ}}_{\text{targ}}$. Before considering the process by which these A^{PZ} nucleons aggregate to form clusters and free particles, one has first to take into account the fact that their momentum distribution can be modified by in-medium nucleon-nucleon collisions.

2. *In-medium nucleon-nucleon collisions*

Indeed, at intermediate energies, nucleons belonging to the participant zone (PZ) experience hard in-medium nucleon-nucleon collisions. Let us call x_{coll} the average number of collisions per participant from the incoming projectile, we thus have for the total number of collisions

$$N_{\text{coll}} = x_{\text{coll}} \times \min\left(A^{\text{PZ}}_{\text{proj}}, A^{\text{PZ}}_{\text{targ}}\right). \tag{3}$$

For a symmetric system considered here, $A^{\text{PZ}}_{\text{proj}} = A^{\text{PZ}}_{\text{targ}}$. The N_{coll} collisions are treated by considering at random a nucleon from the projectile and a nucleon from the target belonging to the participant zone. The elastic scattering is then performed using a fitted free nucleon-nucleon angular distribution. For $p+p$ and $n+n$ collisions, the distribution is isotropic, while for $n+p$, the differential cross section is borrowed from Ref. [11]:

$$\frac{d\sigma}{d\Omega}(E_{\text{lab}},\theta) = \frac{17.42}{1 + 0.05\left(\text{E}^{0.7}_{\text{lab}} - 15.5\right)} \times \exp\left[\alpha\left(\cos^2\theta + \sin^2\frac{\theta}{7} - 1.0\right)\right],$$

with $\alpha = 0.125(E^{0.54}_{\text{lab}} - 4.625)$ for $E_{\text{lab}} \leqslant 100$ MeV, and $\alpha = 0.065(36.65 - E^{0.58}_{\text{lab}})$ for $E_{\text{lab}} > 100$ MeV. Note that the value of α quoted in the original paper is wrong and has been corrected here in agreement with the authors. Figure 1 shows the center-of-mass momentum distributions of the nucleons in the overlap zone (here in the case $b = 0$) before and after collisions for various values of $x_{\text{coll}} = 1.0$, 2.0, and 5.0. The transverse distributions p_x and p_y are enlarged and the longitudinal distributions p_z are damped and may overlap although for the lower values of x_{coll} the two distributions keep a memory of the entrance channel, meaning that full thermalization has not occurred. However, for $x_{\text{coll}} = 5.0$, the two distributions totally overlap.

It turns out that the number of collisions has little influence on the kinematics of fragments. The main effect concerns free nucleons. The value of x_{coll} has been fixed by comparison with the measured proton angular distribution as displayed in Fig. 2.

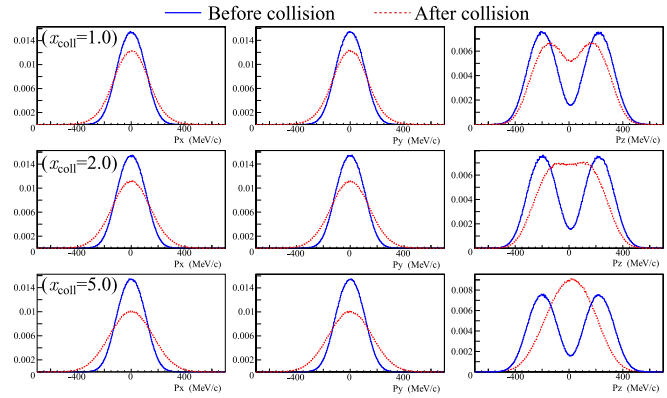

FIG. 1. Normalized center-of-mass momentum distributions of participant nucleons before (blue solid line) and after (red dashed line) nucleon-nucleon collisions for different values of x_{coll}. Left: x axis; middle: y axis; and right: z axis corresponding to the beam axis.

The best agreement between the model and the experimental data is obtained for values of x_{coll} between 1 and 2.

Although x_{coll} is here considered as a free parameter, it is possible to have a rough estimation of its value on the basis of the free nucleon-nucleon cross section, $\sigma^{\text{free}}_{NN}$, using the following parametrization [12]:

$$\sigma_{nn} = \sigma_{pp} = \left(\frac{10.63}{\beta^2} - \frac{29.92}{\beta} + 42.9\right)\text{ mb}, \tag{4}$$

$$\sigma_{np} = \sigma_{pn} = \left(\frac{34.10}{\beta^2} - \frac{82.2}{\beta} + 82.2\right)\text{ mb}, \tag{5}$$

where $\beta = v_{\text{rel}}/c$ is the relative reduced velocity between the two interacting nucleons.

For $E_{\text{beam}} = 95$ MeV/nucleon, $\sigma^{\text{free}}_{NN} = (\sigma_{nn} + \sigma_{np})/2 = (32.04 + 80.25)/2 = 56.15$ mb. The free cross section is corrected by the final-state interaction also known as the Pauli

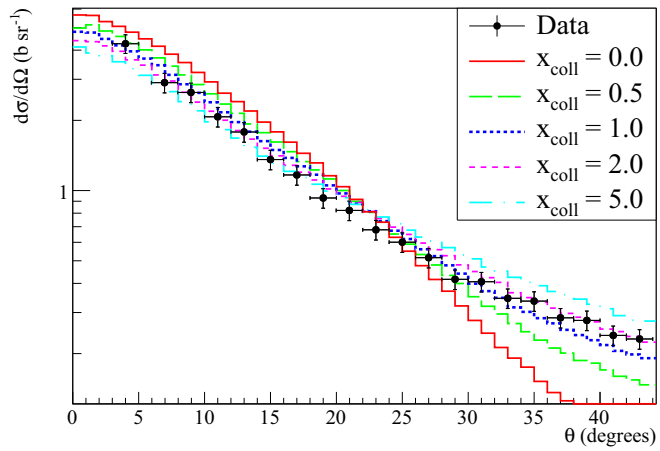

FIG. 2. Angular distributions of the protons for the reaction $^{12}\text{C} + ^{12}\text{C}$ at 95 MeV/nucleon for different values of x_{coll}.

blocking factor $\alpha_{\rm Pauli}$ which can be parametrized as [12]

$$\alpha_{\rm Pauli} = \begin{cases} 1 - \frac{7}{5}\xi & \text{for } \xi \leqslant \frac{1}{2}, \\ 1 - \frac{7}{5}\xi + \frac{2}{5}\xi\left(2 - \frac{1}{\xi}\right)^{5/2} & \text{for } \xi > \frac{1}{2}, \end{cases} \quad (6)$$

where $\xi = E_F/E$, $E_F = 38$ MeV is the Fermi energy and E is the average kinetic energy of the incident nucleon (95 MeV). This gives $\alpha_{\rm Pauli} = 0.44$ and $\sigma_{NN}^{\rm medium} = \alpha_{\rm Pauli}\,\sigma_{NN}^{\rm free} = 24.8$ mb.

For $b = 0$, the number of collisions per incident nucleon writes

$$x_{\rm coll} = \frac{1}{A}\int_0^{R_{\rm max}} 2\pi r\, dr \left(\sum_{i=1}^{A} i e^{-N_r}\frac{N_r^i}{i!}\right) 2\rho_0\sqrt{R_{\rm max}^2 - r^2}, \quad (7)$$

where N_r is the mean number of collisions at a radial distance r for a single incoming nucleon of the projectile along a tube across the target:

$$N_r = 2\rho_0\,\sigma_{NN}^{\rm medium}\sqrt{R_{\rm max}^2 - r^2}. \quad (8)$$

For $A = 12$ (^{12}C+^{12}C), $R_{\rm max} = 2.52$ fm [see Eq. (2)], $\rho_0 = 0.168$ fm^{-3}, and $\sigma_{NN}^{\rm free} = 24.8$ mb, we obtain $x_{\rm coll} = 1.48$. Using $\sigma_{NN}^{\rm free} = 28.5$ mb as in [13], $x_{\rm coll} = 1.70$. These values are compatible with the value obtained previously from data comparisons. In the following, the full comparison with the experimental data is performed with $x_{\rm coll} = 1.5$.

3. Random coalescence between participants

Particle production in the overlap zone is now discussed. Many different algorithms have already been proposed in the literature [14–17] in the framework, for instance, of the intranuclear cascade or MCNP (Monte Carlo N-particle). Here, we consider a coalescence process in momentum space. The main idea is to use a stability criterion. This means that we only consider the production of clusters for which the internal relative kinetic momentum of the nucleon with respect to the fragment does not exceed a given value $p_{\rm cut}$ which is a free parameter of the model. In other words, one starts by choosing randomly a nucleon among the PZs. Then, a second one is chosen and the relative momentum $p_{\rm rel}$ is calculated. If $p_{\rm rel}$ is larger than $p_{\rm cut}$, the aggregation does not occur and the nucleon is the seed of a new fragment. Otherwise, a deuteron is produced (in the procedure, we only consider "realistic" clusters thus excluding di-neutrons, di-protons, and larger unstable clusters. The process is iterated by assigning randomly each new nucleon in the process either to an already existing cluster (if possible) or to a new fragment until the end of the procedure. At the end of the process, all nucleons in the participant zone have been attributed to clusters or are considered as free nucleons. Note that we do not consider the aggregation process in real space but only in momentum space. The reason is that nucleons are delocalized and the geometrical size of the overlap region is of the order of the extension of the wavelength of the nucleons. In the following, the results of the model are shown with an optimized value of $p_{\rm cut} = 225$ MeV/c. It turns out that this value is close to the Fermi momentum $\sim$250 MeV/c.

4. Fragment excitation energy

At the end of the coalescence process, the system is left in a state corresponding to a quasiprojectile, a quasitarget, and several fragments or free nucleons in the midrapidity region. Such species are produced in excited states and the excitation energy has to be determined before considering the second step of the model, namely, the deexcitation process. For heavy systems, the decay of large thermalized sources at high excitation energies can be considered with the help of statistical multifragmentation models (see, for instance, [18]). For such a light system as C-C studied here, discrete known excited states are considered. Such states are assumed to be populated thermally and, as such, a temperature has to be defined. As far as the spectators are concerned, the prescription described in [19] is used. The temperature is a function of the impact parameter and is written as

$$T(b) = T_0 - (T_0 - T_{\rm min})\left[\frac{A_{\rm QP}(b)}{A_{\rm proj}}\right] \text{MeV}, \quad (9)$$

where $T_0 = 7.5$ MeV is the temperature for $b = 0$ and $T_{\rm min} = 4.5$ MeV for $b_{\rm max}$. Using an argument of continuity, T_0 is accordingly the temperature for the fragments in the overlap zone. At larger impact parameter, the temperature is interpolated between T_0 and $T_{\rm min}$, the temperature for the most peripheral collisions, according to the number of nucleons inside the quasiprojectile with respect to the initial number of nucleons of the size of the projectile. The same applies for the quasitarget. When showing the comparison with experimental data, the sensitivity of the results of the model with respect to T_0 and $T_{\rm min}$ will be discussed.

Once the temperature is defined for each b, the excitation energy of the species is sampled by Monte Carlo using a thermal assumption:

$$w_i = \left(2J_i^\pi + 1\right)e^{-E_i/T(b)}, \quad (10)$$

where the degeneracy and energy of each discrete level is found in [20]. Note that we thus only consider known discrete states. This is probably at the origin of some discrepancies between the experimental data and the results of the calculation to be discussed later. It would be interesting to extend the level density distribution to higher energies using a continuum approximation but for the present work, such extension has not been done.

At the end of the coalescence procedure, the total energy of the configuration is calculated by taking into account the mass defects, the excitation energies, and the kinetic energies of the whole species. The momentum of each fragment is obtained by adding the momentum of each nucleon belonging to the fragment. Note that considering such a light system as C+C, the Coulombic final-state interaction between the species is not taken into account.

5. Algorithm for the conservation of energy

The procedure described above does not conserve the total energy of the system. A simple algorithm is thus used to respect energy conservation. An exchange process between the produced species is thus applied. Two protons or two neutrons are randomly chosen and exchanged among the fragments.

The total energy of the configuration is recalculated and the following quantity is minimized:

$$X_{\min} = \left| \frac{{}^{A_{\rm targ}}_{Z_{\rm targ}}\Delta + {}^{A_{\rm proj}}_{Z_{\rm proj}}\Delta + \mathrm{T}_{\rm proj}}{\sum_i \left({}^{A_i}_{Z_i}\Delta + \mathrm{T}_i + \mathrm{E}_i^* \right)} - 1 \right|, \tag{11}$$

where ${}^{A_i}_{Z_i}\Delta$ is the mass excess of the nucleus ${}^{A_i}_{Z_i}\mathrm{X}$, T_i the kinetic energy, and E_i^* the excitation energy. The process is iterated until $X_{\min}$ is less than 1%.

B. Exit or decay channel modeling

In the following, the decay model used to deexcite the species is briefly described. It was shown in our last paper [1] that the Fermi breakup model is by far the most suitable model for such a light system as C+C. Therefore, for each excited species produced in the entrance channel with excitation energy E^*, all possible decay channels with species labeled i that are energetically possible are considered. This procedure includes all possible discrete values for the excited states of each fragment i. Let n be the multiplicity of fragments in the considered decay channel. The energy balance for each partition is

$$E_{\rm avail} = Q + E^* - \sum_i^n E_i^*, \tag{12}$$

where E_i^* is one of the possible excited states of fragment i. Q is the binding energy balance. Therefore, when $E_{\rm avail} > 0$, the considered partition is added to the list of all possible partitions which are energetically acceptable. It remains to sample the partitions according to their statistical weight. This is achieved by the usual phase-space integrals [21]. The probability $W(E_{\rm avail},n)$ for each partition is

$$W(E_{\rm avail},n) = \left(\frac{V}{\Omega}\right)^{n-1} \rho_n(E_{\rm avail}), \tag{13}$$

where $\rho_n(E_{\rm avail})$ is the density in the final state. $V = 4\pi r_0^3 A/3$ is the volume of the decaying system with $r_0 = 1.3$ fm. $\Omega = (2\pi\hbar)^3$ is a normalization volume. A is the mass number of the fragment to be deexcited. The density $\rho_n(E_{\rm avail})$ is the product of three terms:

$$\rho_n(E_{\rm avail}) = M_n(E_{\rm avail}) S_n\, G_n. \tag{14}$$

The first term is a phase-space factor:

$$M_n(E_{\rm avail}) = \int_{-\infty}^{+\infty} \cdots \int_{-\infty}^{+\infty} \delta\left(\sum_{i=1}^n \overrightarrow{\mathrm{p}_i} \right) \times \delta\left(E_{\rm avail} + \sum_{i=1}^n m_i - \sum_{i=1}^n \sqrt{\mathrm{p}_i^2 + m_i^2} \right) \prod_{i=1}^n d^3\mathrm{p}_i, \tag{15}$$

where $\overrightarrow{\mathrm{p}_i}$ is the momentum of fragment i.

The second term is a spin factor taking into account the degeneracy of the considered state of fragment i:

$$S_n = \prod_{i=1}^n (2s_i + 1). \tag{16}$$

The last term is the usual combinatorial factor taking into account the multiplicity n_i of each fragment i:

$$G_n = \prod_{j=1}^k \frac{1}{n_j!}. \tag{17}$$

In the nonrelativistic case, Eq. (15) has an analytical solution [21]. The probability writes as

$$W(E_{\rm avail},n) = S_n G_n \left(\frac{V}{\Omega}\right)^{n-1} \left(\frac{\prod_{i=1}^n m_i}{\sum_{i=1}^n m_i} \right)^{3/2} \times \frac{(2\pi)^{3(n-1)/2}}{\Gamma(3(n-1)/2)} E_{\rm avail}^{3n/2-5/2}, \tag{18}$$

where m_i is the mass of fragment i.

The choice of the partition is made by Monte Carlo according to the statistical weight $W(E_{\rm avail},n)$. The sampling of the momenta of each species is performed according to Eq. (15) using the ROOT [22] class TGENOHASESPACE based on the method of Raubold and Lynch [23].

For those fragments produced in the decay channel which are excited, a new iteration is produced until no more excited species are present in the final state. Note that since the system under study is rather light, the Coulomb interaction between all species in the final state is not taken into account. At the end of the deexcitation process, a complete event is produced, boosted in the laboratory frame. The comparison with experimental data is then possible by taking into account the acceptance of the experimental setup.

III. COMPARISONS WITH EXPERIMENTAL DATA

We now come to a comparison of our model with the experimental data obtained at the GANIL facility and presented in [3]. In the experiment, absolute cross sections for light charged particles were measured over large angular and energy ranges. In a further experiment, additional measurements were also performed at 0° for some isotopes [4].

A. Angular differential cross sections

Figure 3 shows the angular distributions as predicted by the SLIIPIE model (histograms). They are compared with the experimental data (points).

The global features of the data are reproduced by the calculation although it is clear that the model particularly underestimates the production of deuterons, tritons, and ^{3}He at very forward angles. This part of the angular distribution is dominated by the decay of the projectile-like fragment. The underestimation is probably due to a lack of decay channels with emission of deuterons, tritons, and ^{3}He. These channels are associated with rather high excitation energies and the fact that excited states in the continuum are not taken into account certainly leads to a lack of production. Since the measurements

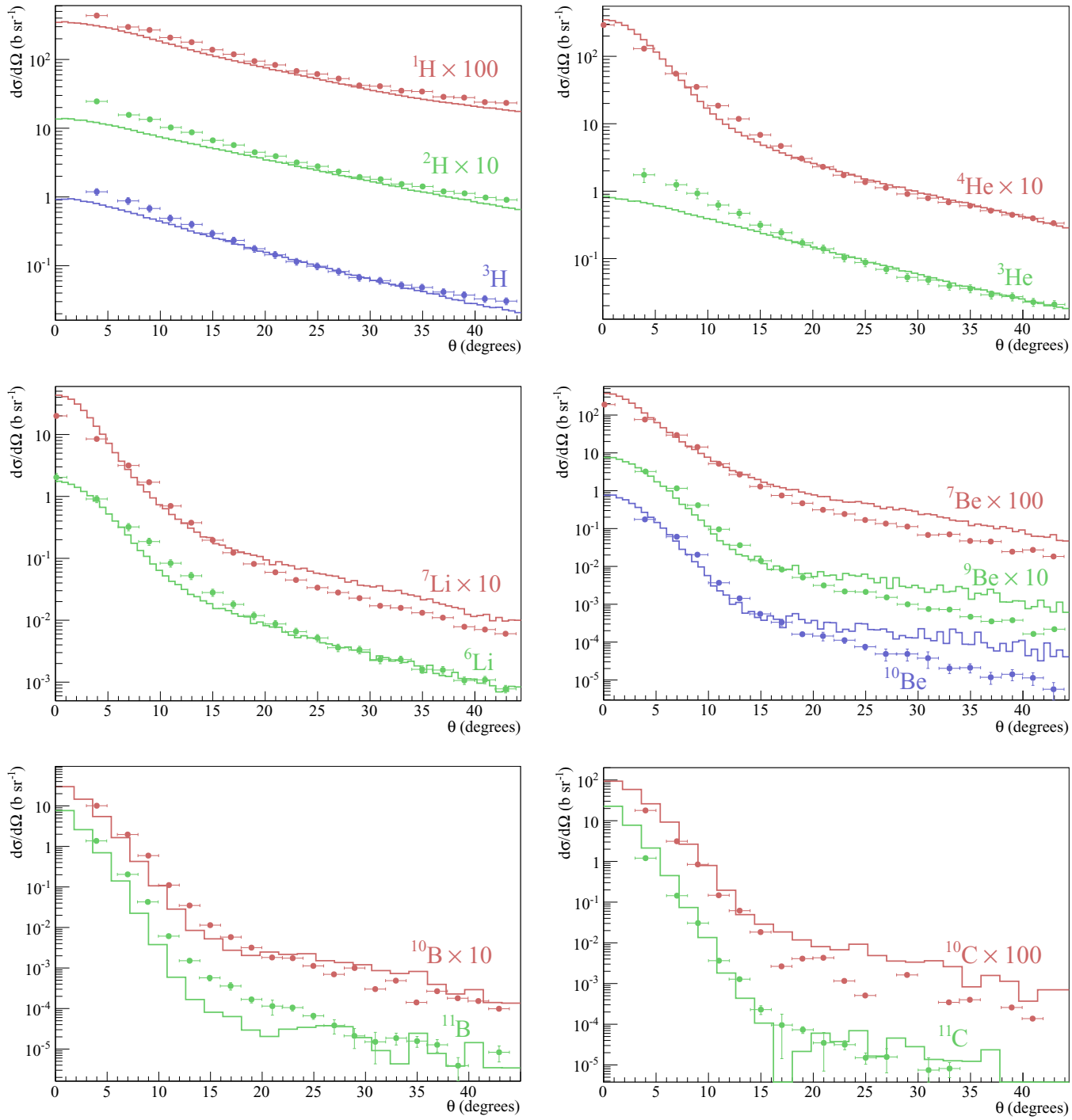

FIG. 3. Angular differential cross sections for various isotopes from $Z = 1$ to $Z = 6$. Points: experimental data from [3,4]. Histograms: results of the SLIIPIE model. For clarity, some values of the cross sections have been multiplied by a factor indicated in each panel.

are limited to angles lower than 45°, the effect on the decay of the target-like fragment is not observed although it is apparent at least in the case of deuterons and tritons at the largest measured angles. Note that the model also slightly underpredicts the production of protons while it gives correct results for α particles.

As far as fragments ($Z > 2$) are concerned, results are quite good. In the model, these cross sections result from the competition between the production of primary species and their subsequent secondary decay. The fact that a rather good agreement is obtained means that the production process is correctly taken into account. This process is essentially governed by geometrical effects since the size of the projectile-like and target-like fragments depends on the size of the participant zone which depends geometrically on the impact parameter. The overestimation of ^{7}Li and ^{7}Be yields at very

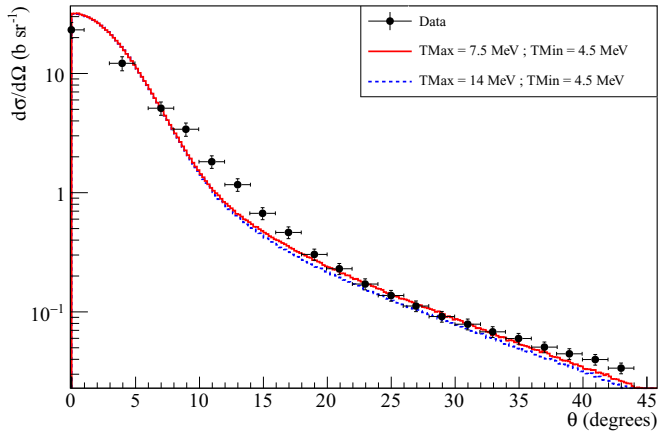

FIG. 4. Angular cross sections for α particles. Points: experimental data from [3,4]. Histograms: results of the SLIIPIE model for two different sets of values of T_0 and $T_{\min}$.

forward angles may be due to the missing decay channels discussed above.

Here, we briefly discuss the influence of the temperature on the results of the model. It turns out that they show very little variations for rather extreme values of T_0 and $T_{\min}$ (see Fig. 4). The reason is that the impact of the temperature is essentially on the population of the excited states of light clusters and not on light-particle production. However, the increase of the temperature towards large values does not change the results because the population of the highly possible discrete excited states rapidly saturates.

B. Double differential cross sections

Figure 5 displays double differential cross sections for some isotopes and various angles. Although discrepancies are observed in the proton spectra at large angles, the agreement for the other displayed isotopes is satisfactory. At small angles, the kinetic energy spectra are dominated by the decay of the projectile-like fragment, and the maxima of the distributions peaked at the beam energy are correctly reproduced. The model is also able to account for the energy distribution of clusters at large angles where the cross section is dominated by processes occurring at midrapidity. Once again, this means that the assumptions regarding the physics in the overlapping zone of the two interacting nuclei is correct. The energy distributions slowly damp as the emission angle increases and the magnitude of the effect is reproduced both in shape and in magnitude.

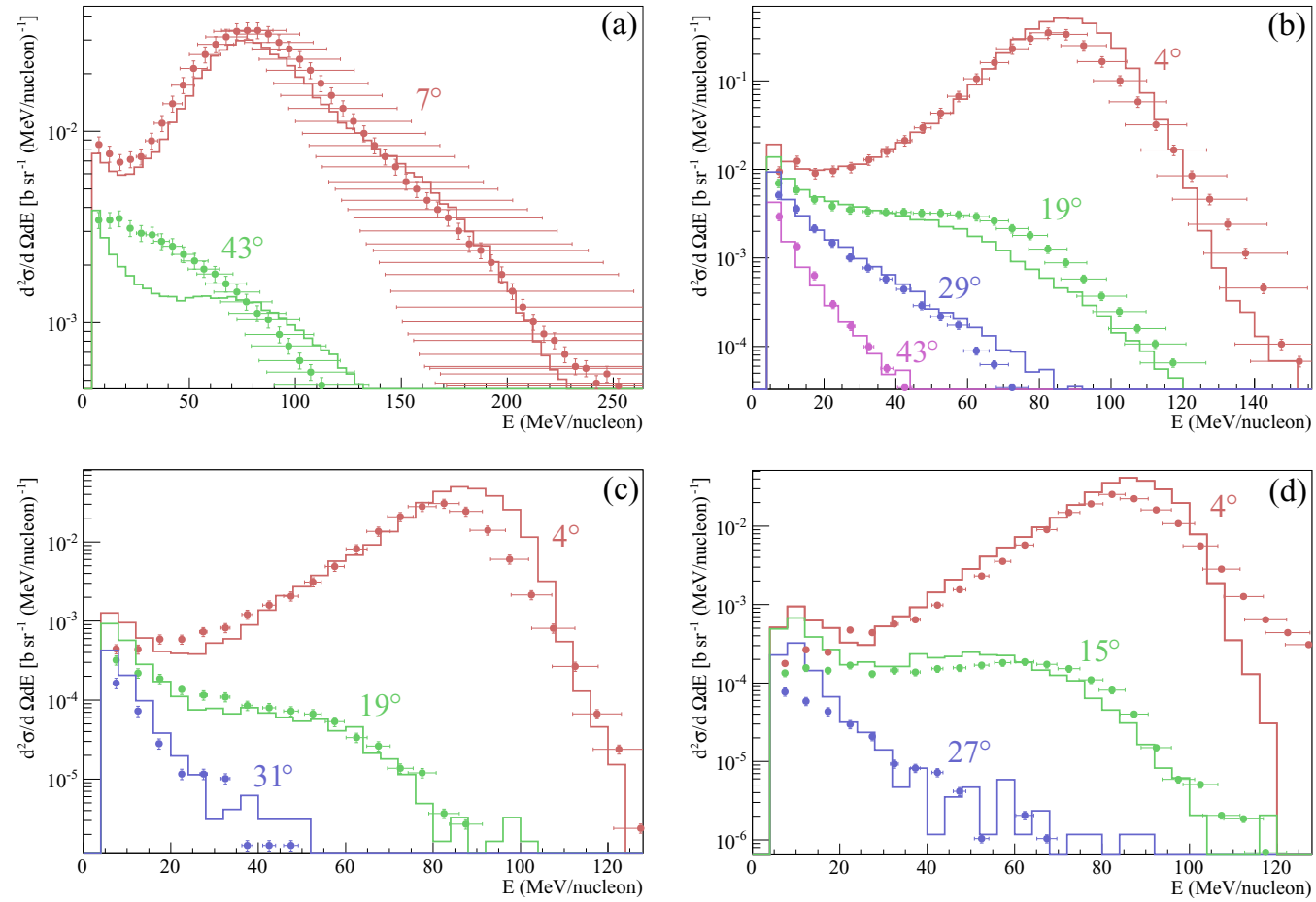

FIG. 5. Double differential cross sections for various isotopes: (a) ^{1}H, (b) ^{4}He, (c) ^{7}Li, and (d) ^{7}Be detected at various angles indicated. The horizontal bars correspond to the uncertainty in the energy measurement (see [3] for more details).

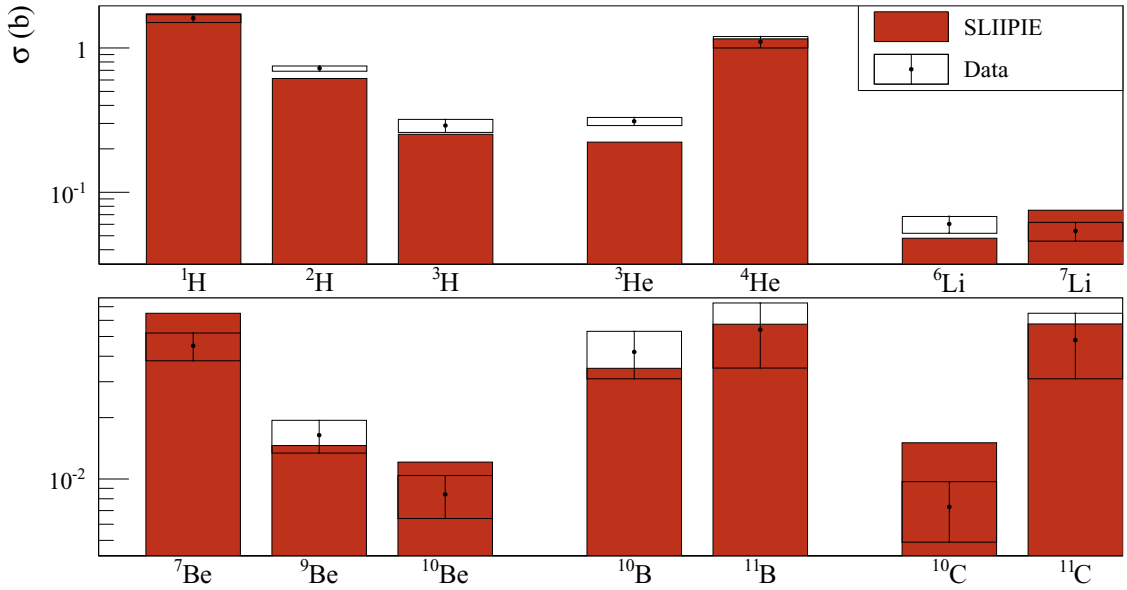

FIG. 6. Total production cross sections for various isotopes. Comparison between the predictions of SLIIPIE and the experimental data.

C. Total production cross sections

Total production cross sections are displayed in Fig. 6. A general agreement between experimental data and the results of the model is achieved for all considered species. A global comparison with other models available in the literature is shown in Fig. 7. The two first models are implemented in GEANT4: the quantum molecular dynamics model [24] (QMD) and the intranuclear cascade of Liege model [25,26] (INCL). These models appeared to be the more predictive of the GEANT4 toolkit for this system in our previous benchmark [1]. The third one, HIPSE [27] (heavy ion phase-space exploration), is a phenomenological model developed to simulate nuclear reactions around Fermi energies. Generally speaking, all models give the correct order of magnitude. In order to be more quantitative, a χ square including all species has been calculated for all considered models with respect to the experimental data. Although none of the models gives very accurate predictions, the SLIPIE results are associated with the best χ square (see Fig. 8).

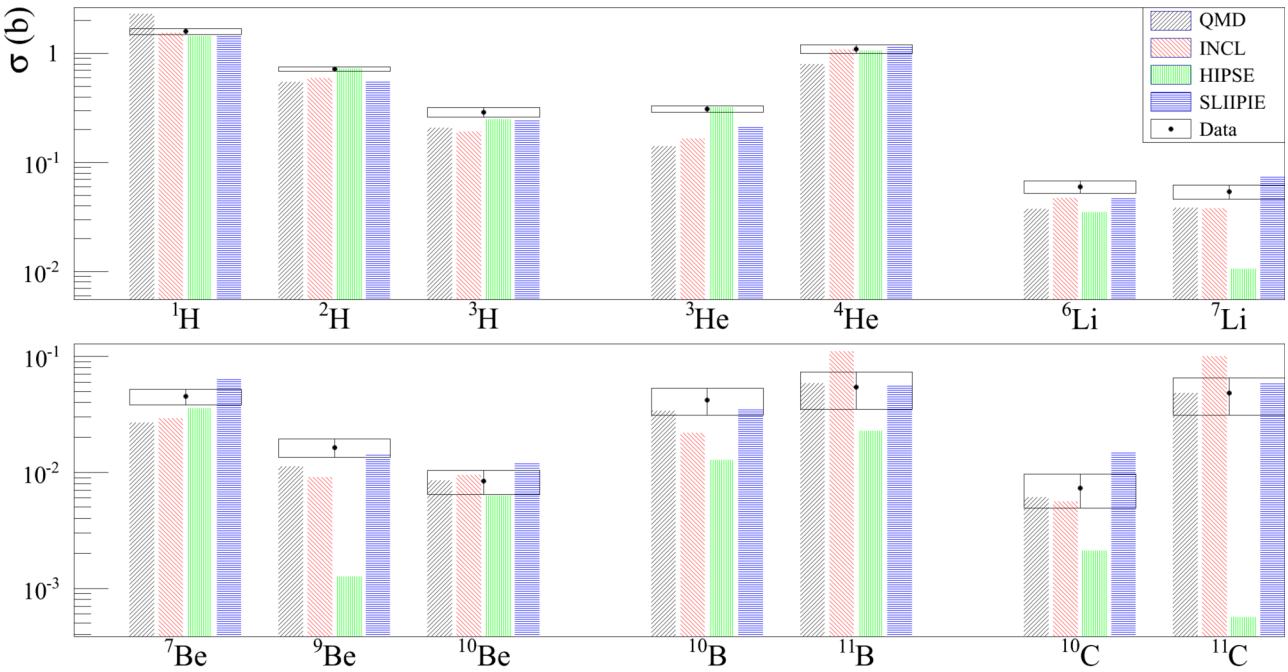

FIG. 7. Comparison between the predictions of the four models and the experimental results for several species.

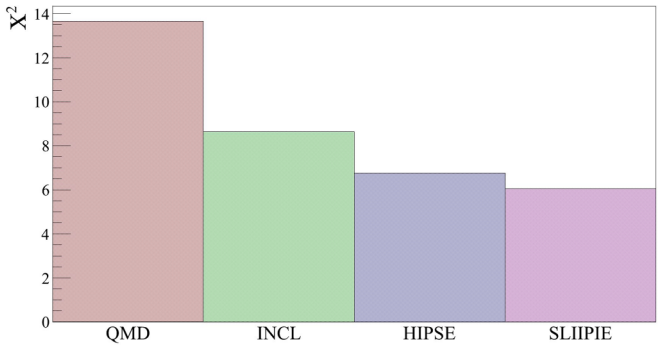

FIG. 8. Comparison of the global χ square for four different models.

IV. CONCLUSION

In this work, we have presented a semimicroscopic model for particle production and compared the results with recent experimental data obtained in C-C reactions at 95 MeV/nucleon. From the rather successful agreement between experimental and calculated data, we may conclude that the main hypotheses of the model are valid. Our results point out a strong memory of the entrance channel characteristics of the reaction, namely, the key role played by the participant-spectator geometrical assumption and the fact that the kinematics of the final products is governed to a large extent by the initial momentum distribution of the two partners of the reaction. This suggests a very fast clusterization process in the overlap region. Such a fast process is difficult to take into account in a fully dynamical description because it requires accounting for a very early coalescence mechanism. Usually, the dynamical models treat cluster production on longer time scales and this could be at the origin of the discrepancies between these models and the experimental data. The "sudden" approximation used in our approach seems to be a key ingredient in reproducing the data, in particular in the midrapidity region. In future works, we plan to extend our model to other systems and other energies.

[1] J. Dudouet, D. Cussol, D. Durand, and M. Labalme, Benchmarking GEANT4 nuclear models for hadron therapy with 95 MeV/nucleon carbon ions, Phys. Rev. C **89**, 054616 (2014).
[2] S. Agostinelli *et al.*, GEANT4 - a simulation toolkit, Nucl. Instrum. Meth. A **506**, 250 (2003).
[3] J. Dudouet, D. Juliani, M. Labalme, D. Cussol, J. C. Angélique, B. Braunn, J. Colin, Ch. Finck, J. M. Fontbonne, H. Guérin, P. Henriquet, J. Krimmer, M. Rousseau, M. G. Saint-Laurent, and S. Salvador, Double-differential fragmentation cross-section measurements of 95 MeV/nucleon ^{12}C beams on thin targets for hadron therapy, Phys. Rev. C **88**, 024606 (2013).
[4] J. Dudouet, M. Labalme, D. Cussol, C. Finck, R. Rescigno, M. Rousseau, S. Salvador, and M. Vanstalle, Zero-degree measurements of ^{12}C fragmentation at 95 MeV/nucleon on thin targets, Phys. Rev. C **89**, 064615 (2014).
[5] C. Dorso and J. Randrup, Early recognition of clusters in molecular dynamics, Phys. Lett. B **301**, 328 (1993).
[6] J. Aichelin, Quantum molecular dynamics: A dynamical microscopic n body approach to investigate fragment formation and the nuclear equation of state in heavy ion collisions, Phys. Rep. **202**, 233 (1991).
[7] P. Chomaz, M. Colonna, and J. Randrup, Nuclear spinodal fragmentation, Phys. Rept. **389**, 263 (2004).
[8] Y. Golubeva, A. Iljinov, E. Paryev, and I. Pshenichnov, Subthreshold η production on nuclei by protons, Z. Phys. A-Hadron Nucl. **345**, 223 (1993).
[9] G. M. Daskalov, M. V. Kazarnovsky, and E. Ya. Parev, The role of quantum effects in the intranuclear-cascade model, Sov. J. Nucl. Phys. **52**, 41 (1990).
[10] H. J. Wollersheim *et al.*, Rare ISotopes INvestigation at GSI (RISING) using gamma-ray spectroscopy at relativistic energies, Nucl. Instrum. Meth. A **537**, 637 (2005).
[11] G. Q. Li and R. Machleidt, Microscopic calculation of in-medium nucleon-nucleon cross sections, Phys. Rev. C **48**, 1702 (1993).
[12] K. Kikuchi and M. Kawai, *Nuclear Matter and Nuclear Reactions*, North-Holland Research Monograph (North-Holland, Amsterdam, 1968).
[13] X.-H. Zeng and L.-X. Ge, Studies of In-Medium Nucleon-Nucleon Collision Cross Section in the Nonrelativistic Energy Region, Commun. Theor. Phys. **26**, 421 (1996).
[14] S. G. Mashnik and L. M. Kerby, MCNP6 fragmentation of light nuclei at intermediate energies, Nucl. Instrum. Meth. A **764**, 59 (2014).
[15] V. Toneev and K. Gudima, Particle emission in light and heavy ion reactions, Nucl. Phys. A **400**, 173 (1983).
[16] H. Schulz, G. Röpke, K. K. Gudima, and V. D. Toneev, The coalescence phenomenon and the Pauli quenching in high-energy heavy ion collisions, Phys. Lett. B **124**, 458 (1983).
[17] D. Mancusi, A. Boudard, J. Cugnon, J. David, P. Kaitaniemi, and S. Leray, Extension of the Liège Intranuclear-Cascade Model to Reactions Induced by Light Nuclei, Phys. Rev. C **90**, 054602 (2014).
[18] J. P. Bondorf, A. S. Botvina, A. S. Ilinov, I. N. Mishustin, and K. Sneppen, Statistical multifragmentation of nuclei, Phys. Rep. **257**, 133 (1995).
[19] S. Mallik, G. Chaudhuri, and S. Das Gupta, Improvements to a model of projectile fragmentation, Phys. Rev. C **84**, 054612 (2011).
[20] http://www.nndc.bnl.gov/chart/.
[21] N. Amelin, Physics and algorithms of the hadronic Monte Carlo event generators. Notes for a developer.CERN/IT/ASD - Geneva, Switzerland and JINR/LHE - Dubna, Russia, 1999 (unpublished).
[22] I. Antcheva *et al.*, ROOT - A C++ framework for petabyte data storage, statistical analysis and visualization, Comput. Phys. Commun. **180**, 2499 (2009).
[23] F. James, *Monte Carlo phase space*, CERN (CERN, Geneva, 1968), p. 41 p, cERN, Geneva, 1 May 1968 .
[24] T. Koi, New native QMD code in Geant4, in *Proceedings, Joint International Conference on Supercomputing in Nuclear Applications and Monte Carlo (SNA + MC2010) : Tokyo, Japan, October 17-21, 2010,* edited by T. Takeda (2011).
[25] P. Kaitaniemi, A. Boudard, S. Leray, J. Cugnon, and D. Mancusi, INCL Intra-Nuclear Cascade and ABLA De-excitation Models in GEANT4, in *Proceedings, Joint International Conference on*

Supercomputing in Nuclear Applications and Monte Carlo (SNA + MC2010) : Tokyo, Japan, October 17-21, 2010, Vol. 2 (2011) p. 788.

[26] A. Boudard, J. Cugnon, J.-C. David, S. Leray, and D. Mancusi, New potentialities of the Liège intranuclear cascade model for reactions induced by nucleons and light charged particles, Phys. Rev. C **87**, 014606 (2013).

[27] D. Lacroix, A. Van Lauwe, and D. Durand, Event generator for nuclear collisions at intermediate energies, Phys. Rev. C **69**, 054604 (2004).